Origin of Magnetism in radiative stars

Thesis project

Juan Pablo Hidalgo

Supervisor : Dr. Dominik Schleicher

Universidad de Concepción.

November 5, 2022

Stellar structure

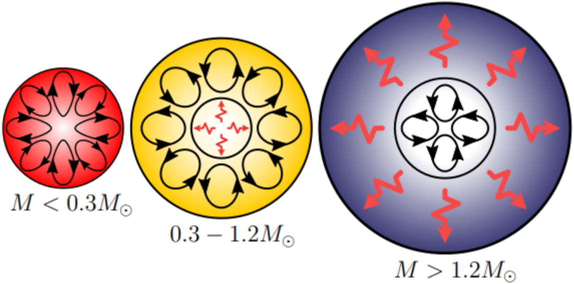

Figure: Diagram of convective and radiative zones for different ranges of stellar masses. Stars with $M \lesssim 0.3M_\odot$ are fully convective, intermediate mass stars have a radiative zone on its core have a radiative zone on its core, and it gets larger as the mass increases. And finally, stars with $M \gtrsim 1.2M_\odot$ are radiative with a convective core (produced by the CNO cycle) (Padmanabhan, 2001).

Astrophysical Dynamos

We refer to a *dynamo* as any process of amplification and maintenance of magnetic fields inside a plasma.

$$\frac{\partial \vec{B}}{\partial t} = \vec{\nabla} \times (\vec{u} \times \vec{B}) + \eta \nabla^2 \vec{B}$$

These processes are most likely to occur inside the convection zones (see Brandenburg & Subramanian 2004), where $u \neq 0$.

Radiative zone?

Ap and Bp stars ($1.5\ M_\odot$ to $6 M_\odot$) have observable magnetic fields up to 34 kG! (Babcock, 1960).

How is this possible?

Possible explanations

There are some theories of how this magnetic field is generated:

- **The dynamo is driven by the convective core of the star:** Augustson et al. (2016).

How is this possible?

Possible explanations

There are some theories of how this magnetic field is generated:

- **The dynamo is driven by the convective core of the star:** Augustson et al. (2016).
- **Fossil field surviving from the early stages:** Braithwaite & Nordlund (2005).

How is this possible?

Possible explanations

There are some theories of how this magnetic field is generated:

- **The dynamo is driven by the convective core of the star:** Augustson et al. (2016).
- **Fossil field surviving from the early stages:** Braithwaite & Nordlund (2005).
- **Shear-driven dynamo in the radiative zone:** Interaction of helical flows and shear, at high R_m (Tobias & Cattaneo, 2013).

How is this possible?

Possible explanations

There are some theories of how this magnetic field is generated:

- **The dynamo is driven by the convective core of the star:** Augustson et al. (2016).
- **Fossil field surviving from the early stages:** Braithwaite & Nordlund (2005).
- **Shear-driven dynamo in the radiative zone:** Interaction of helical flows and shear, at high R_m (Tobias & Cattaneo, 2013).
- **MHD instabilities.**

The model (1)

In this project we will perform 3D MHD simulations of:

- A massive early-type star with a convection core, to explore the core dynamo scenario.

The model (1)

In this project we will perform 3D MHD simulations of:

- A massive early-type star with a convection core, to explore the core dynamo scenario.
- A fully radiative star, to test the fossil field theory looking for stable configurations.

The model (1)

In this project we will perform 3D MHD simulations of:

- A massive early-type star with a convection core, to explore the core dynamo scenario.
- A fully radiative star, to test the fossil field theory looking for stable configurations.

Using:

The Pencil Code

It is a highly modular high-order finite-difference code for compressible non-ideal MHD (Pencil Code Collaboration et al., 2021)

The model (2)

Solving the following equations:

$$\frac{\partial \vec{A}}{\partial t} = \vec{u} \times \vec{B} - \eta \mu_0 \vec{J} \tag{1}$$

$$\frac{D \ln \rho}{Dt} = -\vec{\nabla} \cdot \vec{u} \tag{2}$$

$$\frac{D\vec{u}}{Dt} = -\vec{\nabla}\Phi - \frac{1}{\rho}\left(\vec{\nabla}p - \vec{\nabla} \cdot 2\nu\rho\boldsymbol{S} + \vec{J} \times \vec{B}\right) - 2\vec{\Omega} \times \vec{u} + \vec{f}_d \tag{3}$$

$$T\frac{Ds}{Dt} = -\frac{1}{\rho}\left[\vec{\nabla} \cdot (\vec{F}_{\mathrm{rad}} + \vec{F}_{\mathrm{SGS}}) + \mathcal{H} - \mathcal{C}\right] + 2\nu\boldsymbol{S}^2 + \mu_0\eta J^2 \tag{4}$$

where $D/Dt = \partial/\partial t + \vec{u} \cdot \vec{\nabla}$ is the advective derivative, also $\vec{B} = \vec{\nabla} \times \vec{A}$, the relation between $\vec{J}$ and $\vec{B}$ is given by the Ohm's law $\vec{J} = \vec{\nabla} \times \vec{B}/\mu_0$ and the explicit heating and cooling terms, are extracted from Käpylä (2021).

The model (3)

We will model a star of radius R, inside a box of side $l = 2.2R$, choosing different rotation rates Ω_0 based on the Coriolis number ($\mathrm{Co} \sim 1$, $\mathrm{Co} \sim 2$, $\mathrm{Co} \sim 10$), where $\vec{\Omega} = (0, 0, \Omega_0)$.

The model (3)

We will model a star of radius R, inside a box of side $l = 2.2R$, choosing different rotation rates Ω_0 based on the Coriolis number ($\mathrm{Co} \sim 1$, $\mathrm{Co} \sim 2$, $\mathrm{Co} \sim 10$), where $\vec{\Omega} = (0, 0, \Omega_0)$.

Radiative energy transfer

The size of the radiative zone depends directly on the heat conductivity K_{rad}, a quantity that is inversely proportional to the opacity κ of the star. Thus, we assumed a constant profile and different initial values for it, which are listed on Table 1.

The model (4)

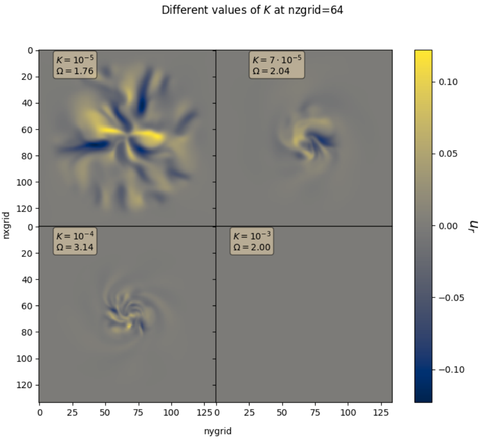

Figure: Snapshots of star-in-a-box simulations using a grid of 128^3, viewing the xy plane in the middle of the z axis. The values of K and Ω are shown on each plot. The colorbar represents the radial component of the flow velocity.

Physical parameters

The physical parameters of the stars that we will be modeling were extracted from MESA-Web, which is the online version of the MESA code (Paxton et al., 2010).

Physical parameters

The physical parameters of the stars that we will be modeling were extracted from MESA-Web, which is the online version of the MESA code (Paxton et al., 2010).

For a 2.18 $M_\odot$ A-type main sequence star, the 1d-model yields:

$$R_* = 2R_\odot \qquad L_* = 23L_\odot$$

$$\rho_* = 56000 \text{ kg/m}^3 \qquad g_* = 150 \text{ m/s}^2$$

Preliminary results (1)

Partially convective:

Run	K	ν	η	Ω	$u_{\rm rms}$	Co	Re	$\mathrm{Re_M}$	$\mathrm{Pr_M}$	$B_{\max}$
	10^{-5}	10^{-3}	$5\cdot10^{-4}$	0	0.111	0	17.68	35.36	2	no dynamo
Sim1	10^{-5}	10^{-3}	$5\cdot10^{-4}$	0.352	0.085	1.32	13.51	27.03	2	0.01652
$\Delta r\sim 1R$	10^{-5}	10^{-3}	$5\cdot10^{-4}$	0.704	0.073	3.06	11.65	23.31	2	-
	10^{-5}	10^{-3}	$5\cdot10^{-4}$	1.760	0.055	10.17	8.77	17.54	2	0.012778
	$4\cdot10^{-5}$	$5.7\cdot10^{-4}$	$5\cdot10^{-4}$	0	0.078	0	21.82	24.84	1.14	no dynamo
Sim2	$4\cdot10^{-5}$	$5.7\cdot10^{-4}$	$5\cdot10^{-4}$	0.245	0.079	0.98	22.17	25.22	1.14	0.012368
$\Delta r\sim 1R$	$4\cdot10^{-5}$	$5.7\cdot10^{-4}$	$5\cdot10^{-4}$	0.489	0.064	2.42	18.03	20.52	1.14	0.016551
	$4\cdot10^{-5}$	$5.7\cdot10^{-4}$	$5\cdot10^{-4}$	1.224	0.055	7.11	15.33	17.45	1.14	-
	$7\cdot10^{-5}$	$2.5\cdot10^{-4}$	$3\cdot10^{-4}$	0	0.195	0	36.97	31.01	0.84	no dynamo
	$7\cdot10^{-5}$	$2.5\cdot10^{-4}$	$3\cdot10^{-4}$	2.044	0.179	1.09	33.93	28.47	0.84	no dynamo
	$7\cdot10^{-5}$	$2.5\cdot10^{-4}$	$3\cdot10^{-4}$	4.087	0.152	2.57	28.79	24.15	0.84	no dynamo
Sim3	$7\cdot10^{-5}$	$2.5\cdot10^{-4}$	$3\cdot10^{-4}$	10.218	0.084	11.63	15.89	13.33	0.84	no dynamo
$\Delta r\sim 0.3R$	$7\cdot10^{-5}$	$2.5\cdot10^{-4}$	$3\cdot10^{-4}$	20.435	0.067	29.23	12.65	10.61	0.84	no dynamo
	$7\cdot10^{-5}$	$2.5\cdot10^{-4}$	$1.5\cdot10^{-4}$	2.044	0.178	1.10	33.72	56.67	1.68	no dynamo
	$7\cdot10^{-5}$	10^{-4}	$9\cdot10^{-5}$	2.044	0.191	1.02	91.17	101.30	1.11	0.0062262
	$7\cdot10^{-5}$	10^{-4}	$9\cdot10^{-5}$	4	0.154	2.48	73.56	81.73	1.11	0.0067169
	10^{-4}	$6.2\cdot10^{-5}$	$8.8\cdot10^{-5}$	0	0.210	0	113.87	79.72	0.7	no dynamo
Sim4	10^{-4}	$6.2\cdot10^{-5}$	$8.8\cdot10^{-5}$	3.140	0.177	1.18	96.19	67.33	0.7	0.0061353
$\Delta r\sim 0.2R$	10^{-4}	$6.2\cdot10^{-5}$	$8.8\cdot10^{-5}$	6.280	0.119	3.52	64.67	45.27	0.7	0.0060869
	10^{-4}	$6.2\cdot10^{-5}$	$8.8\cdot10^{-5}$	15.700	0.109	9.63	59.15	41.40	0.7	0.0056404
	10^{-4}	$6.2\cdot10^{-5}$	$8.8\cdot10^{-5}$	31.401	0.229	9.16	124.31	87.01	0.7	no dynamo

Figure: Summary of all the simulations with convective zone, divided into 4 main groups with different values for the heat conductivity $K_{\rm rad}$ (in code units).

Preliminary results (2)

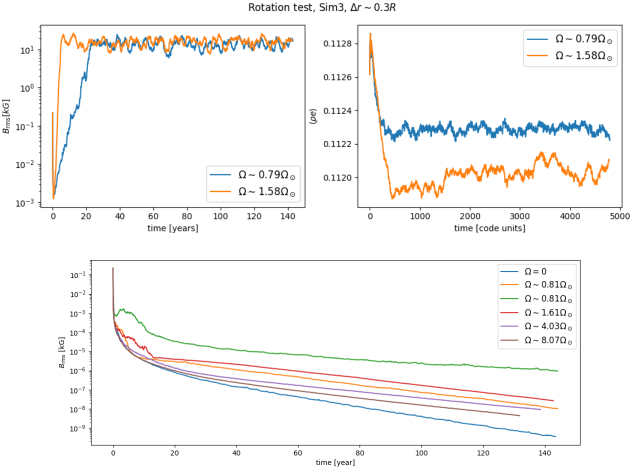

Figure: Root-mean-square magnetic field and mean internal energy vs time from Sim3 $\Delta r \sim 0.3R$.

Preliminary results (3)

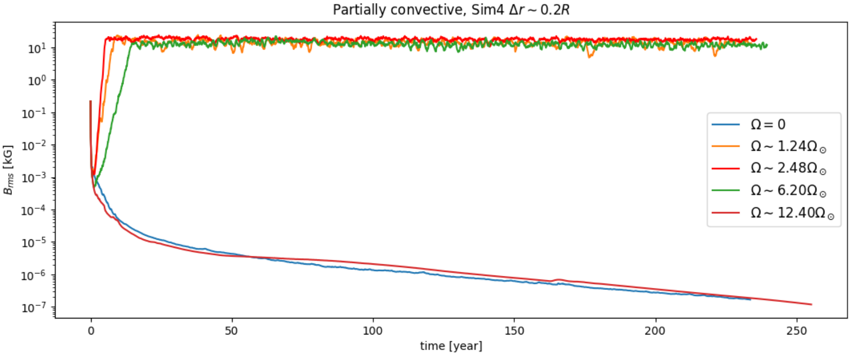

Figure: Root-mean-square magnetic field vs time from Sim4 $\Delta r \sim 0.2R$.

Preliminary results (4)

Sim4 $\Delta r \sim 0.2R$, $\Omega \sim 1.24\Omega_\odot$ (upper), and $\Omega \sim 2.48\Omega_\odot$ (lower):

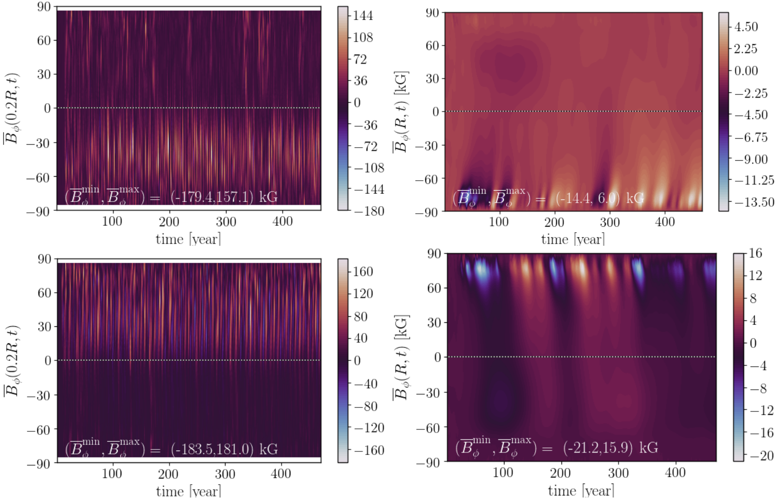

Figure: Azimuthal averaged magnetic field vs time, at different radii ($0.2R$ and $1R$)

Preliminary results (5)

Sim4 $\Delta r \sim 0.2R, \Omega \sim 6.20\Omega_{\odot}$:

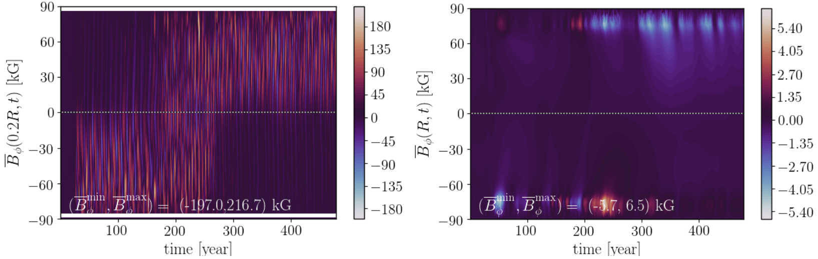

Figure: Azimuthal averaged magnetic field vs time, at different radii ($0.2R$ and $1R$)

References

Augustson K. C., Brun A. S., Toomre J., 2016, , 829, 92

Babcock H. W., 1960, , 132, 521

Braithwaite J., Nordlund A., 2005, Astronomy and Astrophysics, 450

Brandenburg A., Subramanian K., 2004, Phys. Rep., 417

Käpylä P., 2021, Astronomy & Astrophysics, 651

Käpylä P. J., Gent F. A., Olspert N., Käpylä M. J., Brandenburg A., 2020, Geophysical & Astrophysical Fluid Dynamics, 114, 8

Padmanabhan T., 2001, Theoretical Astrophysics - Volume 2, Stars and Stellar Systems, by T. Padmanabhan, pp. 594. Cambridge University Press, July 2001. ISBN-10: 0521562414. ISBN-13: 9780521562416. LCCN: QB801 .P23 2001, vol. II

Paxton B., Bildsten L., Dotter A., Herwig F., Lesaffre P., Timmes F., 2010, The Astrophysical Journal Supplement Series, 192, 3

Pencil Code Collaboration et al., 2021, The Journal of Open Source Software, 6, 2807

Tobias S., Cattaneo F., 2013, Nature, 497, 463

Appendix A

Contributions to momentum and energy in the MHD equations:

- Viscosity

$$\vec{F}_{\text{viscous}} = \frac{1}{\rho}\vec{\nabla}\cdot[2\mu \boldsymbol{S}]$$

with:

$$S_{ij} = \frac{1}{2}(\partial_j u_i + \partial_i u_j) - \frac{1}{3}\delta_{ij}\vec{\nabla}\cdot\vec{u}$$

- Damping of flows

$$\vec{f}_d = -\frac{\vec{u}}{\tau_{\text{damp}}} f_e(r)$$

with:

$$f_e(r) = \frac{1}{2}\left(1 + \tanh\frac{r - r_{\text{damp}}}{w_{\text{damp}}}\right)$$

Appendix A (2)

- SGS entropy flux:

$$\vec{F}_{SGS} = -\chi_{SGS}\rho\vec{\nabla}s'$$

with:

$$s' = s - \langle s \rangle_t$$

- Radiation

$$\vec{F}_{\mathrm{rad}} = -K_{\mathrm{rad}}\vec{\nabla}T$$

- Explicit cooling and heating:

$$\mathcal{C}(\vec{x}) = \rho c_{\mathrm{P}} \frac{T(\vec{x}) - T_{\mathrm{surf}}}{\tau_{\mathrm{cool}}} f_e(r)$$

$$\mathcal{H}(r) = \frac{L_{\mathrm{sim}}}{(2\pi w_{\mathrm{L}}^2)^{3/2}} \exp\left(-\frac{r^2}{2w_{\mathrm{L}}^2}\right)$$

Appendix B

Diagnostics quantities:

$$\mathrm{Re} = \frac{u_{\mathrm{rms}}}{\nu k_R} \qquad \mathrm{Re_M} = \frac{u_{\mathrm{rms}}}{\eta k_R}$$

$$\mathrm{Co} = \frac{2\Omega_0}{u_{\mathrm{rms}} k_R} \qquad \mathrm{Pr_M} = \frac{\nu}{\eta}$$

where $k_R = 2\pi/\Delta r$, and Δr is the size of the convective zone.

All simulations have an initial magnetic field seed, given by a vector potential with a Gaussian profile of amplitude 10^{-9} (*code units*), and were performed on a grid of 128^3.

Physical Units

The Pencil Code expresses all the relevant quantities in code units, so to give them physical meaning it is required to do some conversions:

$$[x] = \left(\frac{R_*}{R_{\text{sim}}}\right) \qquad [t] = \left(\frac{\Omega_{\text{sim}}}{\Omega_*}\right)$$

$$[u] = \left(\frac{\Omega_* R_*}{\Omega_{\text{sim}} R_{\text{sim}}}\right) \qquad [B] = \left[\frac{\mu_0 \rho_* (\Omega_* R_*)^2}{\mu_{\text{sim}} \rho_{\text{sim}} (\Omega_{\text{sim}} R_{\text{sim}})^2}\right]^{1/2}$$

where (see Appendix A of Käpylä et al. 2020):

$$\frac{\Omega_{\text{sim}}}{\Omega_*} = L_{\text{ratio}}^{1/3} \left(\frac{g_{\text{sim}}}{g_*} \frac{R_*}{R_{\text{sim}}}\right)^{1/2}$$

Work-plan

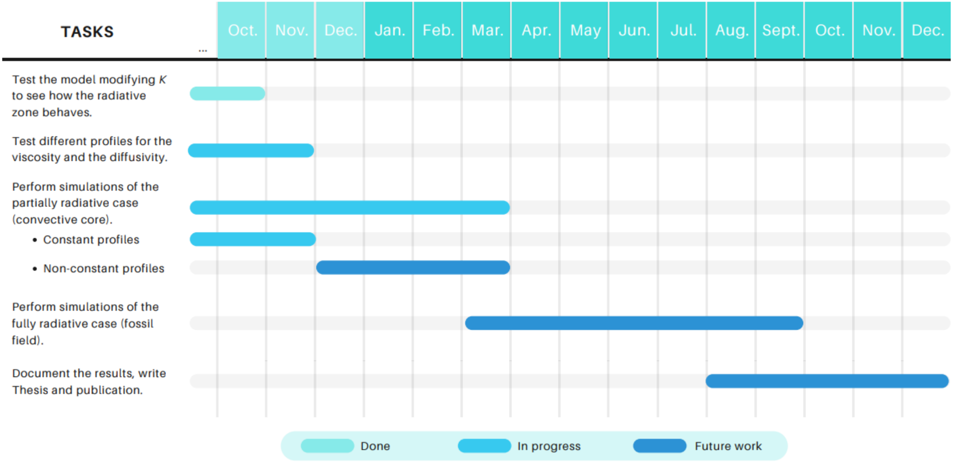
TASKS
...
Oct.
Nov.
Dec.
Jan.
Feb.
Mar.
Apr.
May
Jun.
Jul.
Aug.
Sept.
Oct.
Nov.
Dec.
Test the model modifying K to see how the radiative zone behaves.
Test different profiles for the viscosity and the diffusivity.
Perform simulations of the partially radiative case (convective core).
• Constant profiles
• Non-constant profiles
Perform simulations of the fully radiative case (fossil field).
Document the results, write Thesis and publication.
Done
In progress
Future work